A hybrid approach for pricing American options under the Heston model

Bolujo Joseph Adegboyegun

Department of Mathematical Sciences

Ekiti State University, Nigeria

bja998@uowmail.edu.au

Abstract

Pricing contemporary financial derivatives often require solving multidimensional partial differential equations with mixed derivatives. This paper presents an efficient hybrid approach to directly prescribes the dynamics of American option problems under the Heston stochastic volatility model. The algorithm developed involves trading the roles of financial variables which permit the problem to be solved inversely. The convergence of the algorithm is studied using a variational inequality approach, and we examine the solutions accuracy by comparison with those from existing methods. Furthermore, we explore the effects of time-dependent volatility on the optimal exercise prices.

AMS subject classification: 91G20, 91G30, 91G80

Keywords: The Heston model; American options; Inverse finite elements; Finite differences.

1 Introduction

The Black-Scholes partial differential equation [4] laid the foundations for modern derivatives pricing. However, the assumptions made in the Black-Scholes model are now known to be overly restrictive. The assumption of a fixed volatility in the Black-Scholes model over the tenure of the derivatives is not realistic. In particular, the aftermath of the 1987 global financial crisis was the empirical evidence and economic reasoning which revealed that the distribution of stock return exhibits skewness, kurtosis, and always possesses a negative relationship with implied volatility. This conflicts with the normality assumption made in the Black-Scholes model. Consequently, many derivative pricing models that use the stochastic process for the underlying asset have been developed. These result in a better match to empirically observed results [25]. Examples of more realistic stochastic processes include the jump-diffusion [29], Lévy [23], stochastic volatility (SV) [16], SV jump-diffusion [9], and also the combinations of those that exhibit SV as well as jumps in both the asset price and volatility [11].

The focus of this paper is the Heston stochastic volatility model which has been widely used as the best alternative to the Black-Scholes model because of its analytical tractability for European options. For the American options written on the Heston model, analytical solutions are rarely available. Thus, approximate numerical solutions are often used. Prominent among numerical valuation methods include the tree methods [30], the Fourier-Cosine method [13] and the finite difference methods [19]. The alternating direction implicit (ADI) schemes [33, 17] which are favorite numerical tools to handle multidimensional pricing problems are a direct offshoot of the finite difference methods.

This paper will contribute to the broader field of mathematical finance by extending the applications of the inverse finite element method (iFEM) to the two-factor problem of pricing American put options under the Heston model. Although iFEM was initially used for the treatment of non-linear problems associated with phase change as known in me-

chanics [15, 3], it has, however, been successfully used to price American option problems written on Black-Scholes framework under different formulations [2, 34]. Apparently, the applications of iFEM in quantitative finance have not fully been explored. In the current work, we develop a hybrid algorithm to determine the optimal exercise prices and fair price of American options under the Heston stochastic model. Our technique is similar in some respects to Alexandrou [3], although with additional finite differences to discretize the volatility derivative terms. The method is implemented using the fact that the nodal locations along the volatility direction are fixed while working out the motion of the nodes along the underlying axis.

The rest of the paper is organized as follows. Section 2 reviews the Heston stochastic volatility model, the corresponding PDEs describing American option prices, and the associated boundary conditions. In Section 3, we discuss the hybrid approach in details. Section 4 studies the convergence property of the proposed scheme. While numerical examples and some analyses are presented to demonstrate the efficiency of the scheme in Section 5, concluding remarks are given in the last section.

2 Mathematical formulation

This section introduces the Heston stochastic volatility model and the associated boundary conditions for American put options. Although some authors [21, 33], have studied the Heston model, we still describe it in reasonable details, for the sake of completeness of the paper and ease of reference for the readers. Furthermore, the section contains a brief discussion of the implementation issues concerned when a nonlinear PDE system is solved using the inverse finite element method.

2.1 Heston's stochastic volatility model

The Heston stochastic model is formally defined as the system of stochastic differential equations

$$\begin{cases} dS_t = \mu S_t dt + \sqrt{v_t} S_t dW_1 \\ dv_t = \kappa(\eta - v_t)dt + \xi\sqrt{v_t} dW_2 \\ dW_1 dW_2 = \rho dt, \end{cases} \tag{2.1}$$

where S_t denotes the spot process at time t, v_t the variance at time t, μ the drift rate, and κ the mean reversion speed for the variance. Also, η denotes the mean reversion level for the variance, ξ the volatility of the variance, and $W_i, i = 1, 2$, two Brownian motions with correlation $\rho \in [-1, 1]$. The model for the volatility v_t is known in the financial literature as the Cox-Ingersoll-Ross (CIR) process and mathematical statistics as the Feller process.

Let $P(S, v, t)$ denotes the value of an American put option, with S being the price of the underlying asset with no dividend payment, v being the variance and t is the time. Under the Heston model and using the risk-neutral argument, it can be shown that the value of an American put option, P satisfies the following PDE [14]):

$$\frac{\partial P}{\partial t} + \frac{1}{2} v S^2 \frac{\partial^2 P}{\partial S^2} + \rho\xi v S \frac{\partial^2 P}{\partial S \partial v} + \frac{1}{2}\xi^2 v \frac{\partial^2 P}{\partial v^2} + rS\frac{\partial P}{\partial S} - rP + \left(\kappa(\eta - v) - \lambda\xi\sqrt{v}\right)\frac{\partial V}{\partial v} = 0, \tag{2.2}$$

where λ is the market price of risk, and r is the risk-free interest rate. In this paper, we set λ to zero for simplicity and the extension to the case that λ is non-zero should be straightforward. The parameters ρ, ξ, and κ provide the ability to capture observed features of the market and to produce a wide range of distributions [28]. For examples, the parameter ρ, affects the skewness of the distribution and hence the shape of the implied volatility surface. Also, the parameter ξ, affects the kurtosis of the distribution and the

parameter κ can be interpreted as representing the degree of volatility clustering. These phenomena have repeatedly been observed in the financial market, and a good number of studies have suggested that Heston$'$s model is consistent with the real market.

Notably, Heston [16] derived an analytical solution for the price of European options satisfying Equation (2.2) with associated terminal and boundary conditions. However, the approach adopted could not easily be extended to the case of American options. Therefore, this paper concentrates on the valuation of American put options satisfying Equation (2.2) for which there is no closed-form solution available.

2.2 Boundary conditions

For the parabolic differential equation (2.2) to be solved backward in time, additional constraints/conditions are needed. Because the focus of this work is to provide an efficient solution algorithm for American option problems under the Heston framework, we require the contract set-up to admit a specific solution. Thus, a particular choice of constraints/boundary conditions or parameters would not affect the design of the scheme.

To this end, we denote $G(S) := \max(K - S, 0)$, the so-called payoff function which is independent of v. If at final time T, the value of the stock S is above the strike price K, the option is without value and thus, one would not execute the option. On the other hand, if the value of S is below K, the value of the option is $K - S$. Therefore, at the final T, the value of the option (the terminal condition) reads:

$$P(S, v, T) = \max(K - S, 0) = G(S) \tag{2.3}$$

The boundary conditions with respect to S are easy to justify, in fact, they are similar to those in the Black-Scholes model. The value of an American put option should satisfy

the far-field boundary condition

$$\lim_{S\to\infty} P(S,v,t) = 0, \tag{2.4}$$

which means that when the price of the underlying becomes exceedingly large, a put option becomes worthless. Following the reasoning of Black-Scholes model where similar condition exists, there is a critical asset price, below or equal to which it is optimal to exercise the put option. It can be shown that under the no-arbitrage argument, the boundary conditions at the optimal exercise boundary $S = S_f$ are

$$P(S_f,v,t) = K - S_f, \quad \frac{\partial P}{\partial S}(S_f,v,t) = -1. \tag{2.5}$$

Next, we discuss the boundary conditions along the v direction. Although this is an issue which still remains unclear in the literature, an extensive treatment from both the mathematical and financial points of view was recently provided in [33]. We remark that through consideration of the Fichera function, a boundary condition at $v = 0$ is required when the Feller condition $\kappa\eta \geq \xi^2/2$ is violated. It was argued in [8] that, when required, the appropriate boundary condition to use at this boundary is the payoff function. Moreover, Zhu and Chen [33] advanced that even when the Feller condition is not violated, the solution should converge to the payoff function at this boundary. Therefore, without loss of generality, in the current work, we adopt the boundary conditions along the v direction as stated in [33]. For $v \to 0$, we choose the boundary condition

$$\lim_{v\to 0} P(S,v,t) = \max(K - S, 0). \tag{2.6}$$

The discussion in [8] supported the above choice, and even Zhu and Chen [33] proposed $\lim_{v\to 0} P(S,v,t) = 0$ as a simplified version of Equation (2.6) after they successfully

established that $\lim_{v\to 0} S_f(v,t) = K$.

Finally, one expects that for $v \to \infty$ the value of an American put option reaches the strike price K asymptotically, i.e.,

$$\lim_{v\to\infty} P(S,v,t) = K. \tag{2.7}$$

In summary, the properly-closed PDE system for pricing American put options under the Heston model can be written as

$$\begin{cases} \dfrac{\partial P}{\partial t} + \dfrac{1}{2}vS^2\dfrac{\partial^2 P}{\partial S^2} + \rho\xi vS\dfrac{\partial^2 P}{\partial S\partial v} + \dfrac{1}{2}\xi^2 v\dfrac{\partial^2 P}{\partial v^2} + rS\dfrac{\partial P}{\partial S} - rP + \Big(\kappa(\eta - v)\Big)\dfrac{\partial P}{\partial v} = 0, \\ P(S,v,T) = \max(K-S,0), \\ P(S_f(v,t),v,t) = K - S_f(v,t), \quad \dfrac{\partial P}{\partial S}(S_f(v,t),v,t) = -1, \quad \lim\limits_{S\to\infty} P(S,v,t) = 0, \\ \lim\limits_{v\to 0} P(S,v,t) = \max(K-S,0), \quad \lim\limits_{v\to\infty} P(S,v,t) = K. \end{cases} \tag{2.8}$$

The above PDE system is defined on $S \in [S_f(v,t),\infty)$, $v \in [0,\infty)$, and $t \in [0,T]$. For each $t \in [0,T]$, there exists a stock price, S at which early exercise before final time, T is advantageous. One can show that these values define a continuous curve $S_f(v,t)$. It is *a priori* unknown and therefore defines a free boundary.

2.3 Transformation and localization of domain

Because the governing differential equation in Equation (2.8) is indeed a degenerate parabolic differential equation and to overcome the computational difficulty associated with the moving boundary in the S direction, the following transforms are applied:

$$x = \ln\frac{S}{K}, \quad x_f(v,\tau) = \ln\frac{S_f(v,t)}{K}, \quad u(x,v,\tau) = \frac{P+S}{K} - 1 \quad \text{and} \quad \tau = \frac{\xi^2(T-t)}{2}.$$

The transformed option value $u = u(x, v, \tau)$ then satisfies the dimensionless Heston's equation

$$\begin{cases} \dfrac{\partial u}{\partial \tau} - vq_1 \dfrac{\partial^2 u}{\partial x^2} \dfrac{-2v\rho}{\xi} \dfrac{\partial^2 u}{\partial x \partial v} - v\dfrac{\partial^2 u}{\partial v^2} + (q_1 v - q_2)\dfrac{\partial u}{\partial x} - 2q_1\kappa(\eta - v)\dfrac{\partial u}{\partial v} + q_2 u + q_2 = 0, \\ u(x, v, 0) = \max(e^x - 1, 0), \\ u(x_f(v,\tau), v, \tau) = 0, \quad \dfrac{\partial u}{\partial x}(x_f(v,\tau), v, \tau) = 0, \quad \lim\limits_{x\to\infty} u(x, v, \tau) = e^x - 1, \\ \lim\limits_{v\to 0} u(x, v, \tau) = \max(e^x - 1, 0), \quad \lim\limits_{v\to\infty} u(x, v, \tau) = e^x, \end{cases} \tag{2.9}$$

where $q_1 = 1/\xi^2$ and q_2 is the relative interest rate, which is related to the original risk-free interest rate r by $q_2\xi^2/2$. The system of equations (2.9) is defined on an unbounded domain $\Omega_u^\infty := [0, T\sigma^2/2] \times [x_f, +\infty) \times [0, +\infty)$ i.e., $\Omega_u^\infty := \{(x, v, \tau) \mid x \in [x_f, \infty), v \in [0, \infty), \text{and } \tau \in [0, T\sigma^2/2]\}$.

To proceed with the implementation of the current hybrid method, the range of the option price, u should be known *a priori* and its monotonicity is required along the axis where the moving boundary occurs [3]. From (2.9), one can easily deduce that the option price, u falls within $[0, e^x - 1]$ in the x direction and $[0, e^x]$ in v direction. Furthermore, the monotonically of u is required along the x direction $\forall\ x \in [0, +\infty)$ to ensure a reasonably accurate solution. Following the argument in [34], where similar condition exists, we evaluate

$$\frac{\partial u}{\partial x} = \left(\frac{\partial P}{\partial S} + 1\right)\frac{S}{K}.$$

The value is greater than zero because the delta of an American put option is more than -1 for $S \in [S_f, +\infty)$. Hence, u is strictly monotonically increasing with respect to x for any $x \in (x_f, +\infty)$.

Additionally, the two adopted boundary conditions in the v direction have coincidentally shown the monotonicity of the option price with respect to v as well as its

boundedness:

$$\max(e^x - 1, 0) \leq u(x, v, \tau) \leq e^x.$$

For numerical computation, we need to localize the unbounded domain Ω_u^∞ by defining $\Omega_u := [0, T\sigma^2/2] \times \Omega \subset \mathbb{R}^3$ with the spatial domain $\Omega := [0, x_{\max}] \times [0, v_{\max}] \subset \mathbb{R}^2$. The truncation points $x_{\max}$ and $v_{\max}$ should be sufficiently large to eliminate the boundary effect. Based on the previous estimates [31], we set $x_{\max} = \ln 5$. On the other hand, the highest value of the volatility that has ever been recorded on Chicago Board Options Exchange (CBOE) is only 0.85 [12]. Thus, it is quite reasonable to set $v_{\max} = 1$, and this has also been the case in many previous studies [33, 18]. Upon truncating the computational domain, the range of u becomes $[0, e^{x_{\max}} - 1]$ in the x direction and $[0, e^x]$ in v direction while the monotonicity is retained. In what follows, the construction of the hybrid method is detailed.

3 The hybrid inverse finite element (iFE)/finite difference (FD) method

After successful establishing a closed differential system (2.9), we now focus on the formulation of the hybrid iFE/FD method. The approach follows closely the details described in [3, 34, 2] for the treatment of various non-linear problems, although with an additional final differences. Essentially, the implementation involves interchanging the roles of dependent and independent financial variables, thus allowing the problem to be treated inversely [1]. This requires the boundaries of the elements to remain on "isotherms" of the underlying such that the option value can be specified a *priori* everywhere in the domain. Furthermore, the adopted finite differences elegantly substituted the volatility derivative terms in the governing differential equation with its discretized form, which

permits numerical computations. Finally, with the use of simulated finite elements, we deduce a system of non-linear equation. The solution of the resulting equation through the Newton iterations then reveals the correct location of the free boundary.

For the implementation of the hybrid iFEM/FD approach, we first deal with the time derivative term contained in (2.9). We begin with

$$\frac{du}{d\tau} = \frac{\partial u}{\partial \tau} + \frac{\partial u}{\partial x}\frac{\partial x}{\partial \tau} + \frac{\partial u}{\partial v}\frac{\partial v}{\partial \tau}, \tag{3.1}$$

where $\frac{du}{d\tau}$ is a total derivative, i.e. is the rate of change of the option price at a node. By the concept of iFEM, the option price is distributed and kept constant at all times at the computational nodes, $\frac{du}{d\tau} = 0$. Therefore,

$$\frac{\partial u}{\partial \tau} = -\frac{\partial u}{\partial x}\frac{\partial x}{\partial \tau} - \frac{\partial u}{\partial v}\frac{\partial v}{\partial \tau}. \tag{3.2}$$

In the problem defined above,the mesh along the x-direction is not fixed, but moves with velocity $V_1 = \frac{dx}{d\tau}$. Whereas, the nodal locations along the v-direction are fixed, and thus, the term $\frac{dv}{d\tau} := V_2$ can be determined straightforwardly.

Next, the velocity of the mesh V_1 is approximated by first order finite difference, i.e.,

$$V_1 \approx V_{\text{mesh}} = \frac{x_{\tau+\Delta\tau} - x_\tau}{\Delta\tau} \tag{3.3}$$

Adopting the approximation (3.3), the governing differential equation (2.9) becomes

$$\begin{aligned} &vq_1\frac{\partial^2 u}{\partial x^2} + \frac{2v\rho}{\xi}\frac{\partial^2 u}{\partial x \partial v} + v\frac{\partial^2 u}{\partial v^2} + (q_2 - q_1 v - V_{\text{mesh}})\frac{\partial u}{\partial x} \\ &+ 2q_1\kappa(\eta - v - V_2)\frac{\partial u}{\partial v} - q_2 u - q_2 = 0. \end{aligned} \tag{3.4}$$

Although the numerical treatment of V_{mesh} could affect the accuracy of the final results but adopting a higher order approximation would reduce the truncation errors due to the

approximation in (3.3). In the current work, we confine our attention to the relatively simple case of first-order difference scheme while we defer the treatment of higher-order approximation formulae to future work.

The discretization along the v direction is performed by placing a set of uniformly distributed grids in the computation domain $[0, v_{\max}]$. We denote the number of steps in the v direction by N_v and the step size is defined as $\triangle v = \frac{v_{\max}}{N_v}$. The value of the unknown function u at a grid point along v direction is thus denoted by

$$u^{\tau}_{x,i} \approx u(x, v_i, \tau) = u(x, i\triangle v, \tau),$$

where $i = 0, \ldots, N_v$.

The discretization needs to be conducted in the interior domain $\Omega_v = \{i\triangle v \mid i = 1 \ldots N_v - 1\}$ to approximate the first and second-order spatial derivatives using the standard forward difference schemes

$$\begin{aligned} \frac{\partial u}{\partial v} &\approx A_i = \frac{u^{\tau}_{x,i+1} - u^{\tau}_{x,i}}{\triangle v}, \\ \frac{\partial^2 u}{\partial v^2} &\approx B_i = \frac{u^{\tau}_{x,i+1} - 2u^{\tau}_{x,i} + u^{\tau}_{x,i-1}}{(\triangle v)^2}, \end{aligned} \tag{3.5}$$

At the boundary $\partial\Omega_v = \{i\triangle v \mid i = 0, N_v\}$, the boundary conditions $u^{\tau}_{x,0} = 0$ and $u^{\tau}_{x,\triangle v N_v} = e^x$ are simply incorporated into the discrete equation. With Equation (3.5), the differential equation (3.4) can be written as

$$\begin{aligned} &v_i q_1 \frac{\partial^2 u_i}{\partial x^2} + \frac{2v_i\rho}{\xi}\frac{\partial A_i}{\partial x} + v_i B_i + (q_2 - q_1 v - V_{\text{mesh}})\frac{\partial u_i}{\partial x} \\ &+ 2q_1\kappa(\eta - v_i - V_2)A_i - q_2 u_i - q_2 = 0, \end{aligned} \tag{3.6}$$

which is a system of PDE to be solved. Again, one should recall that all parameters except x are constant real values in Equation (3.6) for each i. At each i, we need to numerically

solve Equation (3.6) for $v = v_i = ih$ where h is the constant v step. For simplicity, we drop the subscript $i's$ hereafter.

Following the traditional finite element method, a residual equation can be constructed as

$$\begin{aligned} R(x) = \int_0^{x_{\max}} \Bigg[& vq_1 \frac{\partial^2 u}{\partial x^2} + \frac{2v\rho}{\xi}\frac{\partial A}{\partial x} + vB + (q_2 - q_1 v - V_{\text{mesh}})\frac{\partial u}{\partial x} \\ & + 2q_1\kappa(\eta - v - V_2)A - q_2 u - q_2)\Bigg]\varphi \, dx = 0, \end{aligned} \tag{3.7}$$

the solution of which is identical to the one of (3.6) in the weak sense. Here, φ is the trial function.

Following the use of divergence theorem, the residual $R(x)$, becomes

$$\begin{aligned} R(x) = \int_0^{x_{\max}} \Bigg[& - vq_1 \frac{\partial u}{\partial x}\frac{\partial \varphi}{\partial x} + \frac{2v\rho}{\xi}A\varphi - \frac{2v\rho}{\xi}A\frac{\partial \varphi}{\partial x} + vB\varphi + (q_2 - q_1 v - V_{\text{mesh}})\varphi\frac{\partial u}{\partial x} \\ & + 2q_1\kappa(\eta - v - V_2)\varphi A - q_2\varphi u - q_2\varphi\Bigg] \, d\Omega. \end{aligned} \tag{3.8}$$

We now proceed to discretize residual equation (3.8) with respect to the space variable x in terms of linear finite elements. For this purpose, we partition the computational domain $[0, x_{\max}]$ into N_x line elements, each of which is mapped isoparametrically into a basic line element with limits $-1 \leq \xi \leq 1$.

Now, expressing u in terms of a finite element basis function as

$$u = \sum_{i=1}^{p} w_i(\tau)\varphi_i(\xi) = (\varphi_i, \ldots, \varphi_p)W^n, \tag{3.9}$$

where W^n is the vector of the nodal values associated with the nth element, i.e.,$W^n = (W_1 \ldots W_p)'$ with the subscripts being the local numbers, and p is the total number of the nodal values of this element.

By substituting (3.9) into (3.8), we obtain the matrix form for the residual of the nth element as

$$R^{(n)}(x) = k^{(n)}W^{(n)} - q^{(n)}, \tag{3.10}$$

where

$$k^{(n)}(i,j) = \int_{-1}^{1} \left(vq_1 \frac{\varphi_i^{'}\varphi_j^{'}}{J_b} + (q_2 - q_1 v - V_{\text{mesh}})\varphi_i^{'}\varphi_j - q_2\varphi_i\varphi_j J_b \right) d\xi, \quad i,j = 1 \ldots p$$

,

$$q^{(n)}(i) = \int_{-1}^{1} \left(M\varphi_i J_b + \varphi_i^{'} \right) d\xi, \quad i = 1 \ldots p$$

and $M = \frac{2v\rho}{\xi}A + vB - q_2 + 2q_1\kappa(\eta - v - V_2)A$.

The term J_b is the stretch factor between x and ξ coordinates. It is the determinant of the Jacobian matrix of the mapping between the coordinate systems. For the linear shape function, $J_b = 1/2$. Using the solid mechanics terminology, $k^{(n)}$ is the so-called element-stiffness matrix, which characterizes the behavior of the element, whereas $q^{(n)}$ is the applied (or external) element generalized-load vector, defined by the element potential energy [27].

Upon specifying the appropriate boundary conditions, the assembling of the element matrices in Equation (3.10) yields

$$R = KW - Q, \tag{3.11}$$

where W is the vector of the known nodal values of the entire domain, K is the constrained master stiffness matrix involving the unknown locations of the underlying asset, and Q represent the vector of forcing term.

To find the location of the underlying asset at each time step, we modify the Newton's algorithm discussed by Zhu and Chen [34]. More specifically, we create an additional loop to handle the finite difference discretization of the volatility derivative terms. Moreover, The Jacobian of the Newton-Raphson procedure is saved using an element-by-element storage and solved by an iterative method based on a modification of the biconjugate gradient stabilized method. The derivatives of the residual equations (3.11) are obtained with respect to the unknown nodal locations x. For the converged results, usually, two to three iterations in the Newton-Raphson procedure are necessary at each time step, and the solution advances to the next time step when all unknowns converge to the stopping criterion set to a relative error of 10^{-4}.

4 The convergence of the algorithm

In this section, we discuss the convergence analysis of the current hybrid approach. This is achieved by providing the error estimate for the nth time steps of the resulting discrete finite element solution. After implementing the finite differences which remove the volatility-dependent terms in the governing differential equation, we reformulate the resulting system as a linear complementarity problem. Then, we establish the weak convergence to the Heston model in the underlying space.

At each time step n, it is not difficult to show that the option pricing problem (2.8) after eliminating the volatility derivative terms is equivalent to the following linear com-

plementarity problem

$$\begin{cases} (\mathcal{L}u - \Lambda).(u - g) = 0, \\ u - g \geq 0, \\ \mathcal{L}u - \Lambda \geq 0, \\ u = \psi \text{ on the boundary}, \end{cases} \tag{4.1}$$

where $g = \max(e^x - 1, 0)$, $\mathcal{L}$ is a partial differential operator defined as

$$\mathcal{L} = vq_1 \frac{\partial^2}{\partial x^2} + (q_2 - q_1 v - V_{\text{mesh}}) \frac{\partial}{\partial x} - q_2 I,$$

and

$$\Lambda = q_2 - vB - 2q_1\kappa(\eta - v - V_2)A - 2v\rho\frac{\partial A}{\partial x}.$$

The problem (4.1) is defined on an infinite domain $\Omega := (\infty, +\infty)$. In practice, we cannot solve the LCP over the whole real number line. So, we truncate the infinite domain into the finite interval, i.e., $\Omega_k := [x_{\min}, x_{\max}]$. Further, we set $x_{\max} = \ln 5$ to ensure consistency with the truncation described in the previous section. As pointed out in [20], this truncation of the domain will only bring inconsequential error in the pricing of American options. On the other hand, $x_{\min}$ here is set to be sufficiently small to eliminate the boundary effect. It is expected that if the desired error estimate of (2.9) is finally derived through that of (4.1), the value of $x_{\min}$ will not affect the former, as a result of the domain of (2.9) being a subset of Ω_k containing $x_{\min}$. However, for symmetric purposes, some published works set $x_{\min} = -x_{\max}$, and we have adopted same in this case.

With the truncated domain Ω_k, first, we derive the equivalent variational form of (4.1) to obtain the desired error estimate.

Lemma 4.1. *(**Variational inequality**) At each time step, the linear complementary problem (4.1) is equivalent, in the weak sense, to solving for a $w \in \mathcal{K}$, such that for all*

$\phi \in \mathcal{K}$, the inequality $a(w, \phi - w) \geq (g, \phi - w)$ holds, where

$$\mathcal{K} := \{\phi \in H_1(\Omega) : \phi \geq 0,\ \phi(\partial\Omega) = 0\}, \quad \Pi = q_2 - q_1 v - V_{mesh},$$

$$\begin{aligned} a(w, \phi - w) =& v q_1 \int_{\Omega_k} \frac{\partial w}{\partial x} \frac{\partial(\phi - w)}{\partial x}\ d\Omega_k - \frac{1}{2} \int_{\Omega_k} \Pi \left[\frac{\partial w}{\partial x}(\phi - w) - w \frac{\partial(\phi - w)}{\partial x} \right]\ d\Omega_k \\ &+ \int_{\Omega_k} \left(q_2 + \frac{1}{2} \frac{\partial V_{mesh}}{\partial x} \right)(\phi - w) w\ d\Omega_k \end{aligned}$$

and

$$\begin{aligned} (g, \phi - w) =& - v q_1 \int_{\Omega_k} \frac{\partial \psi}{\partial \psi} \frac{\partial(\phi - w)}{\partial x}\ d\Omega_k + \int_{\Omega_k} \Pi \frac{\partial \psi}{\partial x}(\phi - w)\ d\Omega_k - \int_{\Omega_k} q_2 \psi(\phi - w)\ d\Omega_k \\ &- \int_{\Omega_k} \Big[q_2 - vB - 2q_1 \kappa(\eta - v - V_2) A \Big](\phi - w)\ d\Omega_k + \int_{\Omega_k} 2 v \rho A \frac{\partial(\phi - w)}{\partial x}\ d\Omega_k \end{aligned}$$

Proof. Let $L_2(\Omega_k)$ be the usual space of Lebesgue measurable and square integrable functions on $\Omega = [x_{\min}, x_{\max}]$ and denote by $H_0^1(\Omega_k)$ the Sobolev space of first-order weak derivatives. We define $\mathcal{K} \subset H_0^1(\Omega_k)$ as

$$\bar{\mathcal{K}} := \{\phi \in H_1(\Omega) : \phi \geq g,\ \phi(x) = g(x), \forall x \in \partial\Omega\}, \tag{4.2}$$

where the inequality sign means to hold pointwise $\forall\ x \in \Omega_k$. Let $\phi \in \bar{\mathcal{K}}$ be any test function and $u \in \bar{\mathcal{K}}$ be a solution of problem (4.1). For all $\phi \in \mathcal{K}$, we have $\phi - g \geq 0$. We multiply the third equation in (4.1) by $\phi - g$ (which does not change in sign) and integrate over Ω_k, yielding $\int_{\Omega_k} \mathcal{L}u - \Lambda).(\phi - g)\ d\Omega_k \geq 0$. Subtraction of the first equation

in (4.1), integrated over Ω_k, that is, $\int\limits_{\Omega_k} (\mathcal{L}u - \Lambda).(u - g)\, d\Omega_k = 0$, yields

$$\int\limits_{\Omega_k} (\mathcal{L}u - \Lambda).(\phi - u)dx \geq 0,$$

thereby eliminating ψ. Furthermore, we apply a transformation $w = u - g$ in order to achieve zero boundary conditions. For this, we need to assume for the moment that g is sufficiently smooth. According to this transformation, we define a new constraint space as

$$\mathcal{K} := \{\phi \in H_1(\Omega) : \phi \geq 0,\ \phi(x) = 0\} \tag{4.3}$$

Therefore, the linear complementarity problem (4.1) is equivalent to finding $w \in \mathcal{K}$ with

$$\int\limits_{\Omega_k} [\mathcal{L}(w + g) - \Lambda].(\phi - w)dx \geq 0.$$

By applying integrating by parts technique, it is now clear that the weak solution of (4.1) is the solution of the following problem. Finding $w \in \mathcal{K}$, such that for all $\phi \in \mathcal{K}$

$$\begin{aligned} &vq_1 \int\limits_{\Omega_k} \frac{\partial w}{\partial x}\frac{\partial(\phi - w)}{\partial x}\, d\Omega_k - \int\limits_{\Omega_k} \Pi\frac{\partial w}{\partial x}(\phi - w)\, d\Omega_k + q_2 \int\limits_{\Omega_k} w(\phi - w)\, d\Omega_k \geq \\ &- vq_1 \int\limits_{\Omega_k} \frac{\partial \psi}{\partial \psi}\frac{\partial(\phi - w)}{\partial x}\, d\Omega_k + \int\limits_{\Omega_k} \Pi\frac{\partial \psi}{\partial x}(\phi - w)\, d\Omega_k - \int\limits_{\Omega_k} q_2\psi(\phi - w)\, d\Omega_k \\ &- \int\limits_{\Omega_k} \Big[q_2 - vB - 2q_1\kappa(\eta - v - V_2)A\Big](\phi - w)\, d\Omega_k + \int\limits_{\Omega_k} 2v\rho A\frac{\partial(\phi - w)}{\partial x}\, d\Omega_k \end{aligned} \tag{4.4}$$

Using the fact that

$$\begin{aligned}\frac{1}{2}\int_{\Omega_k}\Pi\frac{\partial w}{\partial x}(\phi-w)\,d\Omega_k =&\frac{1}{2}\Pi(\phi-w)w\mid_{\partial\Omega_k}-\frac{1}{2}\int_{\Omega_k}\Pi\frac{\partial\Pi}{\partial x}(\phi-w)w\,d\Omega_k-\frac{1}{2}\int_{\Omega_k}w\Pi\frac{\partial(\phi-w)}{\partial x}\,d\Omega_k\\ =&-\frac{1}{2}\int_{\Omega_k}\Pi\frac{\partial\Pi}{\partial x}(\phi-w)w\,d\Omega_k-\frac{1}{2}\int_{\Omega_k}w\Pi\frac{\partial(\phi-w)}{\partial x}\,d\Omega_k,\end{aligned} \tag{4.5}$$

the left-hand side of (4.5) can be written as

$$vq_1\int_{\Omega_k}\frac{\partial w}{\partial x}\frac{\partial(\phi-w)}{\partial x}\,d\Omega_k-\frac{1}{2}\int_{\Omega_k}\Pi\left[\frac{\partial w}{\partial x}(\phi-w)-w\frac{\partial(\phi-w)}{\partial x}\right]d\Omega_k+\int_{\Omega_k}\left(q_2+\frac{1}{2}\frac{\partial Q_x}{\partial x}\right)(\phi-w)w\,d\Omega_k$$

Therefore, at the nth time step, the linear complementary problem (4.1) becomes: solve for $w\in\mathcal{K}$, such that for all $\phi\in\mathcal{K}$, the inequality $a(w,\phi-w)\geq(g,\phi-w)$ is always satisfied. □

Lemma 4.2. *When the sizes of the time step and the elements are sufficiently small, the inequality* $\frac{\partial V_{mesh}}{\partial x}\geq 0$ *holds.*

Proof. The details of proof can be found in [34]. □

Following the reasoning in [34, 26], Lemma 4.2 is proved with the condition that both temporal and spacial step sizes are approaching zero. Thus, it is numerically challenging to identify the δ_1-neighborhood and δ_2-neighborhood of zero for Δt and Δx, respectively. Finally, using Lemma 4.2, the ellipticity of the bilinear form $a(\cdot,\cdot)$ and the boundness of both $a(\cdot,\cdot)$ and (ψ,ϕ) can be achieved. These are essential requirements to establish the error estimate of the finite element solution of the class of problem (4.1).

Theorem 4.3. $a(\cdot,\cdot)$ *is a continuous* $\mathcal{H}^1$*-elliptic bilinear form and* (g,ϕ) *is bounded.*

Proof. According to the definition of $a(\cdot,\cdot)$, it is clear that for all $\phi \in \mathcal{H}^1(\Omega)$,

$$a(\phi,\phi) = vq_1 \int_\Omega \left(\frac{\partial \phi}{\partial x}\right)^2 d\Omega + \int_\Omega \left(q_2 + \frac{1}{2}\frac{\partial V_{\text{mesh}}}{\partial x}\right)\phi^2 \, d\Omega \geq L \int_\Omega \left[vq_1\left(\frac{\partial \phi}{\partial x}\right)^2 + \phi^2\right] d\Omega, =$$
$$L\|\phi^2\|, \left(\text{since } q_2 \text{ and } \frac{\partial V_{\text{mesh}}}{\partial x} \geq 0\right),$$

where L is a positive constant.

Moreover, $\forall\ \varphi, \phi \in \mathcal{H}^1(\Omega)$,

$$a(\varphi,\phi) = \int_\Omega \frac{\partial \varphi}{\partial x}\frac{\partial \phi}{\partial x}\, d\Omega - \int_\Omega M\frac{\partial \varphi}{\partial x}\phi \, d\Omega + \int_\Omega q_2\varphi\phi \, d\Omega \geq \|\varphi\|_1\|\phi\|_1(1 + \|M\|_{\Omega,\infty} + q_2).$$

Therefore, $a(\cdot,\cdot)$ is in a continuous $\mathcal{H}^1$-elliptic bilinear form provided that M is ∞-measurable on the Ω, which is the case here.

On the other hand,

$$(g,\phi) = -\int_\Omega q_2\phi \, d\Omega + \int_\Omega M\phi \, d\Omega - \int_\Omega \frac{\partial g}{\partial x}\frac{\partial \phi}{\partial x}\, d\Omega +$$
$$\int_\Omega \Pi\frac{\partial g}{\partial x}\phi \, d\Omega - \int_\Omega q_2 g\phi \, d\Omega,$$

□

where $N = vB + 2Av\rho 2 + 2q1k[\eta - v - V2]A$ and $\Pi = q_2 - q_1 v - V_{\text{mesh}}$.

Referencing Theorem 4.3 together with the generalized LaxMigram theorem [22, 6], the linear complementary problem (4.1) has a unique solution.

Next, with the linear elements, we have adopted to discretize (4.1) with respect to the space variable x, Ω has been decomposed into uniform line segment with length proportional to a parameter h. We define $V_h \in \mathcal{H}^1(\Omega)$ as the finite element space spanned by the one-dimensional linear basis functions and has vanishing boundary values at the

boundary.

In addition, let

$$\bar{\mathcal{K}_{\langle}} := \{\phi_h \in V_h, \phi_h \geq 0, \text{and } \phi_h = 0 \text{ on } \partial\Omega\}.$$

The discrete version of (4.1) is to find $w_h \in \bar{\mathcal{K}_{\langle}}$, such that $\forall \phi \in \bar{\mathcal{K}_{\langle}}$, $a(w_h, \phi_h - w_h) \geq (g, \phi_h - w_h)$ holds pointwise. Also, the existence and uniqueness of the discrete solution is guaranteed by the generalized LaxMilgram theorem, applied to finite dimensional spaces [6].

On the other hand, the error analysis for the discrete solution of (4.1) is $\| w - w_h \|_{\mathcal{H}^1(\Omega)} = \mathcal{O}(h)$ as long as $g \in L^2(\Omega)$. This reasoning follows that of Brezzi et al. [5], where similar conditions exist. Thus, with respect to the $L^2(\Omega)$ norm, and using the explicit Euler algorithm, the error analysis for the discrete solution of problem (4.1) is

$$\| w - w_h \|_{\text{Ł}^2[\Omega\times(0,T))]} = \mathcal{O}(h^2 + \triangle t) \tag{4.6}$$

5 Numerical results and discussion

This section presents numerical results of the hybrid iFE/FD algorithm for pricing American options written on Heston's stochastic volatility model. First, we investigate whether the computed solution can be validated. Since there is no exact solution of Problem 2.8 in closed form, we compare the option price from the current hybrid approach with some of the existing numerical solutions. In addition, the section presents some graphical results to illustrate the effects of time-dependent volatility on the optimal exercise boundary of American options.

5.1 Option prices

Here, we compare the performance of the hybrid iFE/FD method with various finite difference methods' pricing results given by Clark & Parrott [8], Zvan et al. [35], Oosterlee [24] and Zhu and Chen [33]. The model parameters are presented in Table 1. These parameters are chosen to permit direct comparison with the reference works.

Table 1: Model parameters

Strike price K (\$)	10
Interest rate r	0.1
Correlation parameter ρ	0.1
Mean reversion level η	0.16
Expiry time T	0.25
Mean reversion rate k	5
Initial stock prices S_0 (\$)	8,. . . ,12

For our computation, we fix the number of points in the v coordinate as $N_v = 50$, with a varying number of time and space steps: $N_\tau = N_x = 50, 75, 100$. We calculate two sets of American put options with different parameters. The option values are presented in Tables 2 and 3 at fives stock prices $S = 8, 9, 10, 11, 12$, and for variance values $v_0 = 0.25$ and $v_0 = 0.0625$. We have used different discretization grids to study the accuracy of the numerical solutions. The prices reported in [35, 8, 24, 33] are also shown in these tables for comparisons. It can be seen that even with the most coarse grid $N_\tau = N_x = 50$, the error is only about 10^{-2}. The prices obtained with the finest grid are reasonably close to the ones in [35, 8, 24, 33], and the error is about 10^{-3}. This confirms that our numerical solution does converge to that of the original nonlinear PDE.

Next, we graph the option value versus the stock price at different time to expiry as some readers may wish to see the result in graphical forms. Depicted in Figure 1 is the option price, $P(S, v, \tau)$ as a function of S with fixed variance $v = 0.25$ at four instants, $\tau = 0$, $\tau = 0.1$ (Year), $\tau = 0.5$ (Year) and $\tau = 1$ (Year). Clearly, the option

Table 2: Comparison of the computed option prices with the reference solutions at $v_0 = 0.25$

N_x, N_τ	$S_0 = 8$	$S_0 = 9$	$S_0 = 10$	$S_0 = 11$	$S_0 = 12$
$50, 50$	2.0968	1.4581	0.8918	0.5493	0.2932
$75, 50$	2.0444	1.3325	0.7941	0.4470	0.2423
$75, 75$	2.0780	1.3329	0.7952	0.4477	0.2426
$100, 75$	2.0781	1.3333	0.7956	0.4480	0.2427
$100, 100$	2.0783	1.3347	0.7958	0.4481	0.2428
Ref. [33]	2.0781	1.3337	0.7965	0.4496	0.2441
Ref. [8]	2.0733	1.3290	0.7992	0.4536	0.2502
Ref. [24]	2.0790	1.3340	0.7960	0.4490	0.2430
Ref. [35]	2.0784	1.3337	0.7961	0.4483	0.2428

Table 3: Comparison of the computed option prices with the reference solutions at $v_0 = 0.0625$

N_x, N_τ	$S_0 = 8$	$S_0 = 9$	$S_0 = 10$	$S_0 = 11$	$S_0 = 12$
$50, 50$	1.9829	1.1067	0.5190	0.2136	0.0818
$75, 50$	1.9836	1.1075	0.5193	0.2136	0.0821
$75, 75$	1.9979	1.1075	0.5199	0.2136	0.0820
$100, 75$	2.0000	1.1076	0.5199	0.2136	0.0821
$100, 100$	2.0000	1.1076	0.5120	0.2137	0.0821
Ref. [33]	2.0000	1.0987	0.5082	0.2106	0.0861
Ref. [8]	2.0000	1.1080	0.5316	0.2261	0.0907
Ref. [24]	2.0000	1.1070	0.5170	0.2120	0.0815
Ref. [35]	2.0000	1.1076	0.5202	0.2138	0.0821

price is a decreasing function of stock price. As it gets closer to the expiration of the option, i.e. $\tau \to 0$ or $t \to 1$ (year), the option price becomes closer to the payoff function $\max(K - S, 0)$. In fact, when $\tau = 0$, the option price is just the S axis starting from $S = \$10$, since $S_f(v, 0) = \$10$ implies that $P(S, v, \tau) = 0$ for all $S \geq \$10$.

5.2 Optimal exercise prices

So far, we have only presented some detailed results on the option value. For the pricing of American options, it is far more crucial to determine the optimal exercise price than

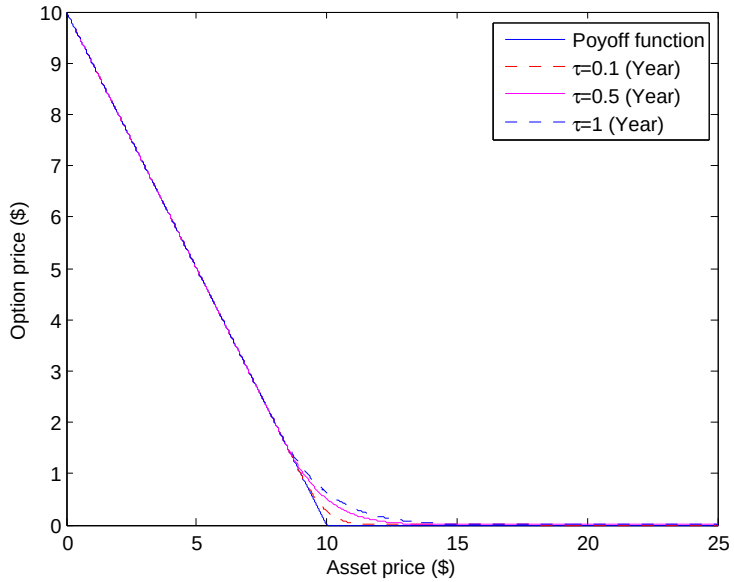

Figure 1: Option prices at different times to expiration. Model parameters are $k = 5, \eta = 0.16, \rho = 0.1, r = 0.1, T = 1, K = 10, \xi = 0.9, v_0 = 0.25$

the option price itself. In fact, once the optimal exercise price is accurately determined, the problem becomes a fixed boundary problem and the determination of the option price is straightforward [32]. In what follows, we present some graphs to illustrate the effects of time-dependent volatility on the optimal exercise price.

The optimal exercise price $S_f(v, \tau)$ with different fixed variance values is shown in Figure 2. As clearly shown, the optimal exercise price is a monotonically decreasing function of $T - t$ or a monotonically increasing function of t. As the time, t approaches the expiration time, T of the option, the optimal exercise price rises sharply towards the strike price $K = \$10$. At $t = T$ or $\tau = 0$, $S_f(v, \tau) = K$, as we expected. Figure 2 also shows that the rate of change of $S_f(v, \tau)$ is much larger near the expiration time than when the option contract is far from expiration. In fact, it is because of this large rate of change of the optimal exercise price near the expiration time that most numerical algorithms have difficulties dealing with the singular behaviour of the optimal exercise

price near $t = T$ or $\tau = 0$. However, in this case, the algorithm is designed to deal with this problem as the location of the optimal exercise price at expiry is known *a priori* and is already included in the algorithm.

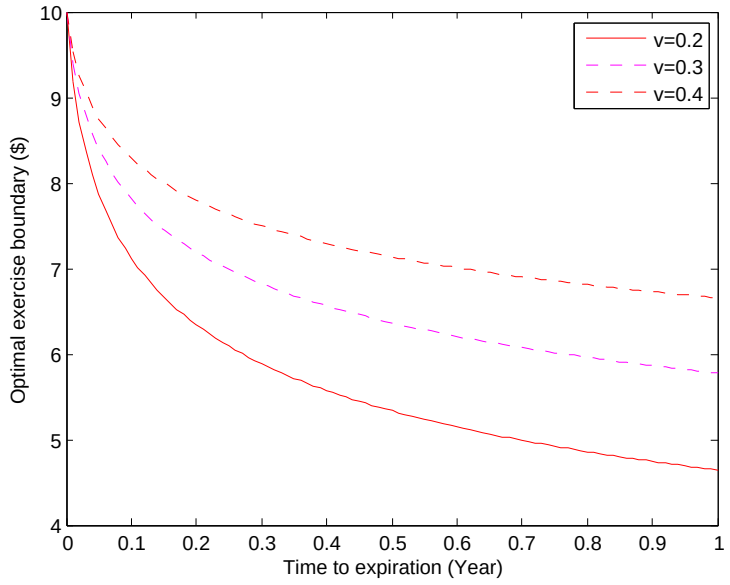

Figure 2: Optimal exercise prices with different volatility values. Model parameters are $k = 5$, $\eta = 0.16$, $\rho = 0.1$, $r = 0.1$, $T = 1$, $K = 10$, $\xi = 0.3$, $N_\tau = N_x = 100$

Depicted in Figure 3 is a graph of $S_f(v, \tau)$ with different fixed time to expiration τ. As clearly shown in Figure 3, the optimal exercise price is a monotonically decreasing function of v and $S_f(v, \tau)$ approaches the strike price as v approaches zero.

shown [33, 7] that whether or not the Feller condition is violated, the solution converges to the same value at the boundary where $v = 0$. Therefore, considering the two scenarios, we graph the optimal exercise prices using the grid resolution $N_\tau X N_x = 10X40$ for each case. The model parameters are the same with those used in Figure 2 except using $\xi = 0.3$ when the Feller condition is satisfied and $\xi = 2$ when it is violated. The figure shows that even though the Feller condition is violated, the results converge to the same value as $v \to 0$.

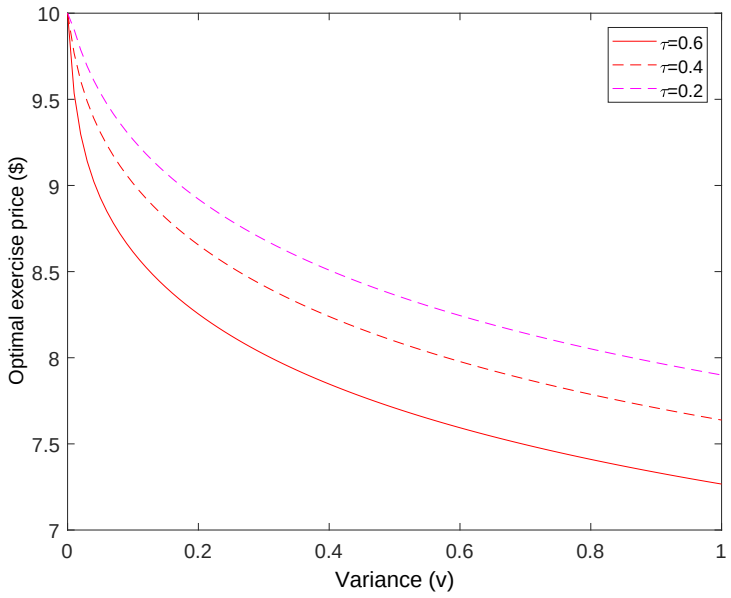

Figure 3: Optimal exercise prices with different time to expiration. Model parameters are $k = 5$, $\eta = 0.16$, $\rho = 0.1$, $r = 0.1$, $T = 1$, $K = 10$, $\xi = 0.9$, $N_\tau = N_x = 100$

5.3 Efficiency and convergence of the algorithm

Attempt is made here to compare the computational cost of the hybrid method with a known method, predictor-corrector method [33], in the literature. The tested examples is chosen with the parameter values $k = 1.5$, $\eta = 0.16$, $\rho = 0.1$, $r = 0.1$, $T = 1$, $K = 10$. These values are consistent with the model parameters of the referenced work in order to ensure a fair comparison.

Table 4 compares the runtime measures as the computational cost of the current hybrid method with the predictor-corrector method at various grid resolutions. As shown in the table, the major set back of the current algorithm is its high computational cost. The time required to evaluate the results is quite high and the CPU memory used is large. However, much of the implementation of the proposed algorithm has been geared toward

proof of concept and no optimization of the code has been attempted. .

Table 4: Comparison of the computational cost of the hybrid method and predictor-corrector scheme

N_x	$N_{/tau}$	N_v	Ref. [33]	Hybrid method
13	25	50	0.8440	418.3720
26	80	50	3.4370	7004.6543
52	250	50	19.5420	423513.7456

Next, we briefly investigate the convergence of our numerical result. We are particularly interested in the convergence properties of the algorithm as the grid is refined. To achieve this, we consider the convergence ratio proposed by D'Halluin et al. [10].

Let $\triangle\tau = h$ and $\triangle x = h$. For all our tests, we simply use as constant step size, h for both temporal and spatial directions. If we then carry out a convergence study by letting $h \to 0$, then we can assume that the error in the solution (at a given node) is $P_N(h) = P_{\text{exact}} + h^{\omega}$, and the convergence ratio is defined as

$$ratio = \frac{P_{N/2} - P_M}{P_{M/4} - P_{M/2}}, \tag{5.1}$$

where P_N denotes here the approximated price obtained with $N = N_x$ number of finite elements. We fixed the number of v steps at $N_v = 50$. For each test, as we double the number of grid points by reducing the time-step and element sizes ($\triangle x = \triangle\tau = 0.02$ on the coarsest grid) in half.

Table 5: Ratio of the price of American put options as the starting point S_0 varies

M	$S_0 = 8$	$S_0 = 8$	$S_0 = 10$	$S_0 = 11$	$S_0 = 12$
50	2.41087	2.73284	3.02986	2.96705	3.28045
100	2.21926	2.37261	2.39418	2.41290	2.43874
200	2.01274	2.11748	2.14439	2.17503	2.16423

In the case of quadratic convergence ($\omega = 2$), the ratio = 4, while for linear convergence ($\omega = 2$), ratio = 2. In Table 5, we show the convergence rate for an American put option

written on Heston′s model using the data in Table 1. The table shows that ratios of the present method are all around 2 and 3, which suggests that the convergence ratio for the current method is linear in both x and τ direction. Moreover, Table 5 shows that the observed ratios are very stable, and this gives an evidence of the stability of the method.

6 Conclusion

In this paper, we have presented a hybrid method for pricing American options written on the Heston model. We establish the convergence by reformulating the discretized problem in a variational form and study the approximation of the option price. The advantage of the proposed algorithm is that it preserves the simplicity and flexibility of the conventional finite element and finite difference methods while allowing the use of full Newton iteration scheme with its inherent quadratic convergence. Various numerical experiments suggest that the current method is comparable with the existing valuation methods. Based on the numerical results, we have also examined the influence of the time-dependent volatility on the optimal exercise prices.

Acknowledgement

We would like to thank Professor Song-Ping Zhu and Dr Xioaping Lu for their useful comments during the preparation of this work.

References

[1] B. J. Adegboyegun. *A further study of the inverse finite element approach for pricing American-style options*. PhD thesis, University of Wollongong, July 2017.

[2] B. J. Adegboyegun. An inverse finite element method for pricing American options under linear complementarity formulations. *Mathematics Applied in Science and Technology*, 10(1):1–17, 2018.

[3] A. N. Alexandrou. An inverse finite element method for directly formulated free boundary problems. *International journal for numerical methods in engineering*, 28(10):2383–2396, 1989.

[4] F. Black and M. Scholes. The pricing of options and corporate liabilities. *The journal of political economy*, pages 637–654, 1973.

[5] F. Brezzi, W. W. Hager, and P.-A. Raviart. Error estimates for the finite element solution of variational inequalities. *Numerische Mathematik*, 28(4):431–443, 1977.

[6] P. G. Ciarlet. *The finite element method for elliptic problems*, volume 40. Siam, 2002.

[7] K. Clarke, N & Parrott. Multigrid for American option pricing with stochastic volatility. *Applied Mathematical Finance*, 6(3):177–195, 1999.

[8] N. Clarke and K. Parrott. Multigrid for American option pricing with stochastic volatility. *Applied Mathematical Finance*, 6(3):177–195, 1999.

[9] M. Creel and D. Kristensen. Abc of sv: Limited information likelihood inference in stochastic volatility jump-diffusion models. *Journal of Empirical Finance*, 31:85–108, 2015.

[10] Y. d'Halluin, P. A. Forsyth, and K. R. Vetzal. Robust numerical methods for contingent claims under jump diffusion processes. *IMA Journal of Numerical Analysis*, 25(1):87–112, 2005.

[11] D. Duffie, J. Pan, and K. Singleton. Transform analysis and asset pricing for affine jump-diffusions. *Econometrica*, 68(6):1343–1376, 2000.

[12] C. B. O. Exchange. The CBOE volatility index-VIX. *White Paper*, pages 1–23, 2009.

[13] C. W. Fang, F & Oosterlee. A fourier-based valuation method for Bermudan and barrier options under Heston's model. *SIAM Journal on Financial Mathematics*, 2(1):439–463, 2011.

[14] J. Gatheral. *The volatility surface: a practitioner's guide*, volume 357. John Wiley & Sons, 2011.

[15] M. Gherlone, P. Cerracchio, M. Mattone, M. Di Sciuva, and A. Tessler. An inverse finite element method for beam shape sensing: theoretical framework and experimental validation. *Smart Materials and Structures*, 23(4):045027, 2014.

[16] S. L. Heston. A closed-form solution for options with stochastic volatility with applications to bond and currency options.

[17] S. Hout, K J & Foulon. ADI finite difference schemes for option pricing in the Heston model with correlation. *Int. J. Numer. Anal. Model*, 7(2):303–320, 2010.

[18] J. Ikonen, S & Toivanen. Efficient numerical methods for pricing American options under stochastic volatility. *Numerical Methods for Partial Differential Equations*, 24(1):104–126, 2008.

[19] J. Ikonen, S & Toivanen. Operator splitting methods for pricing American options under stochastic volatility. *Numerische Mathematik*, 113(2):299–324, 2009.

[20] R. Kangro and R. Nicolaides. Far Field Boundary Conditions for Black-Scholes Equations. *SIAM Journal on Numerical Analysis*, 38(4):1357–1368, 2000.

[21] A. Kunoth, C. Schneider, and K. Wiechers. Multiscale methods for the valuation of american options with stochastic volatility. *International Journal of Computer Mathematics*, 89(9):1145–1163, 2012.

[22] S. Larsson and V. Thome. *Partial differential equations with numerical methods*, volume 45. Springer Science & Business Media, 2008.

[23] P. Nowak and M. Pawłowski. Option pricing with application of levy processes and the minimal variance equivalent martingale measure under uncertainty. *IEEE Transactions on Fuzzy Systems*, 25(2):402–416, 2017.

[24] C. W. Oosterlee. On multigrid for linear complementarity problems with application to American-style options. *Electronic Transactions on Numerical Analysis*, 15(165-185):2–7, 2003.

[25] C. O'SULLIVAN and S. O'SULLIVAN. Pricing European And American Options In The Heston Model With Accelerated Explicit Finite Differencing Methods. *International Journal of Theoretical and Applied Finance*, 16(03):1350015, 2013.

[26] A. Quarteroni and F. Sacco, R & Saleri. *Numerical mathematics*, volume 37. Springer Science & Business Media, 2010.

[27] S. S. Rao. *The finite element method in engineering*. Butterworth-heinemann, 2017.

[28] F. D. Rouah. *The Heston Model and its Extensions in Matlab and C*. John Wiley & Sons, 2013.

[29] R. U. Seydel. Modeling tools for financial options. In *Tools for Computational Finance*, pages 1–82. Springer, 2017.

[30] H. Vellekoop, M & Nieuwenhuis. A tree-based method to price American options in the Heston model. *Journal of Computational Finance*, 13(1):1, 2009.

[31] P. Wilmott, J. Dewynne, and S. Howison. *Option pricing: Mathematical models and computation*. Oxford financial press, 1993.

[32] S.-P. Zhu. On various quantitative approaches for pricing American options. *New Mathematics and Natural Computation*, 7(02):313–332, 2011.

[33] S.-P. Zhu and W.-T. Chen. A predictor-corrector scheme based on the ADI method for pricing american puts with stochastic volatility. *Computers & Mathematics with Applications*, 62(1):1–26, 2011.

[34] S.-P. Zhu and W. T. Chen. An inverse finite element method for pricing American options. *Journal of Economic Dynamics and Control*, 37(1):231–250, 2013.

[35] R. Zvan, P. Forsyth, and K. Vetzal. Penalty methods for American options with stochastic volatility. *Journal of Computational and Applied Mathematics*, 91(2):199–218, 1998.